

REPORT DOCUMENTATION PAGE

AFRL-SR-AR-TR-06-0094

Public reporting burden for this collection of information is estimated to average 1 hour per response, including the time for reviewing instructions, data needed, and completing and reviewing this collection of information. Send comments regarding this burden estimate or any other aspect of this burden to Department of Defense, Washington Headquarters Services, Directorate for Information Operations and Reports (0704-0188-4302). Respondents should be aware that notwithstanding any other provision of law, no person shall be subject to any penalty for failing to valid OMB control number. PLEASE DO NOT RETURN YOUR FORM TO THE ABOVE ADDRESS.

1. REPORT DATE (DD-MM-YYYY) 31-03-2006	2. REPORT TYPE final	3. DATES COVERED (From) 2003-2006
4. TITLE AND SUBTITLE High Performance Organic Materials and Devices		5a. CONTRACT NUMBER
		5b. GRANT NUMBER F49620-03-1-0101
		5c. PROGRAM ELEMENT NUMBER
		5d. PROJECT NUMBER
		5e. TASK NUMBER
		5f. WORK UNIT NUMBER
7. PERFORMING ORGANIZATION NAME(S) AND ADDRESS(ES)		8. PERFORMING ORGANIZATION REPORT NUMBER
Prof. Yang Yang Department of Materials Science and Engineering UCLA 6531 Boelter Hall Los Angeles, CA 90095	Prof. Fredl Wudl Department of Chemistry and Biochemistry UCLA Los Angeles, CA 90095	9. SPONSORING / MONITORING AGENCY NAME(S) AND ADDRESS(ES)
		10. SPONSOR/MONITOR'S ACRONYM(S) AFSOR
		11. SPONSOR/MONITOR'S REPORT NUMBER(S)

12. DISTRIBUTION / AVAILABILITY STATEMENT

Approve for Public Release: Distribution Unlimited

13. SUPPLEMENTARY NOTES

14. ABSTRACT

During our three-year period of time, significant progresses have been achieved in PLEDS, PV cells and memory devices. First, vertical OFET with astonishing device performance was demonstrated: low operating voltage (< 5 V), high current output (> 10 mA, or 4A/cm²), and high ON/OFF ratio (4×10^6). These new devices were operated by modulating charge injection, rather than charge transport. This invention opened a new direction in basic scientific research for organic transistors and their applications. For the first time, an organic transistor which has sufficient power to drive an organic LED was demonstrated. Second, highly efficient polymer solar cells based on a bulk heterojunction of polymer poly(3-hexylthiophene) and methanofullerene was shown. An efficiency of up to 4.4 %, one of the highest numbers published so far, was achieved by controlling the growth rate of the active layer. The high efficiency achieved in this work brings this device one step closer to commercialization. Third, 7,8,10-triphenylfluoranthene, a highly luminescent solid-state blue-emitting small molecule, was synthesized. OLEDs based on this material exhibited external quantum efficiency of 2.48% and electroluminescence efficiency as high as 3.33 cd/A.

15. SUBJECT TERMS

16. SECURITY CLASSIFICATION OF:			17. LIMITATION OF ABSTRACT	18. NUMBER OF PAGES	19a. NAME OF RESPONSIBLE PERSON
a. REPORT	b. ABSTRACT	c. THIS PAGE			19b. TELEPHONE NUMBER (include area code)

Year 2003-2006 Final Report to AFOSR

Project title: High Performance Organic Materials and Devices

Grant Number: F49620-03-1-0101

Program Director: Dr. Charles Lee

PI: Prof. Yang Yang
Department of Materials Science and Engineering
UCLA
6531 Boelter Hall
Los Angeles, CA 90095

Co-PI: Prof. Fredl Wudl
Department of Chemistry and Biochemistry
UCLA
Los Angeles, CA 90095

Date: March 31, 2006

e-mail: yangy@ucla.edu

20060405000

Objectives

Our research objective is to study high performance organic semiconductor materials and their applications. We separate our objectives in following three categories:

1. Novel organic field effect transistors with high current output, low operating voltage and high ON/OFF ratio.
2. Polymer based photovoltaic cells with high power conversion efficiency and low fabrication cost.
3. Pure blue fluorescent materials and organic light-emitting device with high efficiency.

Status of efforts

We are pleased to report to AFOSR that we have achieved significant progress in all the categories of research topics.

First, by using simple thermal vacuum evaporation technique, we successfully fabricated the vertical OFET with astonishing device performance: low operating voltage (< 5 V), high current output (> 10 mA, or $4\text{A}/\text{cm}^2$), and high ON/OFF ratio (4×10^6). These new devices are operated by modulating charge injection, rather than charge transport. This invention opens a new direction in basic scientific research for organic transistors and their applications. **For the first time, we demonstrated that an organic transistor has sufficient power to drive an organic LED.**

Second, we have successfully demonstrated highly efficient polymer solar cells based on a bulk heterojunction of polymer poly(3-hexylthiophene) and methanofullerene. **An efficiency of up to 4.4 %, which was calibrated with the help from National**

Renewable Energy Labs (NREL), Colorado, was achieved by controlling the growth rate of the active layer. Power conversion efficiency of 4.4% is one of the highest published numbers so far for polymer based solar cells. The high efficiency achieved in this work brings this device one step closer to commercialization.

Third, we have synthesized 7,8,10-triphenylfluoranthene, a highly luminescent solid-state blue-emitting small molecule that can be obtained in two steps from commercial starting materials. The OLEDs based on blue-fluorescent 7,8,10-triphenylfluoranthene and its doping property in a host of dipyrenylfluorene derivatives were demonstrated. The devices exhibited pure blue emission with a peak wavelength of 456 nm and Commission International de L'Eclairage coordinate at (0.164, 0.188). **The external quantum efficiency of 2.48% and electroluminescence efficiency as high as 3.33 cd/A were achieved.**

Accomplishments/New findings

1. Vertical OFET with prominent device performance: low operating voltage (< 5 V), high current output (> 10 mA, or 4A/cm²), and high ON/OFF ratio (4×10^6).
2. Ambipolar vertical OFET achieved by inserting a transition metal oxide layer at the source/drain interface. An organic inverter is also demonstrated with a gain of 13.6.
3. High power conversion efficiency achieved for P3HT:PCBM system (4.4 % calibrated with the help from NREL) by self-organization in polymer film.
4. High fill factor (up to 67%), very low device series resistance (1.5 Ω), more than 90% absorption in active layer, and highly balanced carrier transport.

5. High efficient blue-electroluminescence device shows maximum efficiency of 3.33 cd/A and external quantum efficiency of 2.48%.

Personal supported:

Faculty: Yang Yang (PI for the project and responsible for the devices), Fredl Wudl (co-PI, responsible for materials synthesis and processing)

Post-Docs: Liping Ma (invention of high-speed organic diode, and Cu-induced organic memory and high performance vertical organic transistor). Jianhua Wu (theoretical calculation for organic memory, 3 months in 2004), Jun He (some characterizations, 18 month in 2003-2004, half time), Gang Li (polymer solar cells, 2004 – present, half time).

Graduate students: We have a splendid list of students trained under the support from AFOSR. Qianfei Xu (memory device, PhD. 2004), Fang-Chung Chen (solar cell, Ph.D. 2003), Chih-Wei Chu (nanocluster for OFETs, PhD. 2006), and Yan Shao (organic solid solution, PhD 2005) Ryan Chiechi (polymer material synthesis, PhD 2005), William Wei-Jen Hou (polymer solar cells).

List of publications:

1. R. C. Chiechi, R. J. Tseng, F. Marchioni, Y. Yang, and F. Wudl, “Efficient blue electroluminescent devices with a robust fluorophore: 7,8,10-triphenylfluoranthene” *Adv. Mater.* **18**, 325 (2006).
2. R. J. Tseng, R. C. Chiechi, F. Wudl, and Y. Yang “Highly efficient 7,8,10-triphenylfluoranthene -doped blue organic light-emitting diodes for display application” *Appl. Phys. Lett.*, **88**, 093512 (2006).

3. Jinsong Huang, Gang Li, Elbert Wu, Qianfei Xu, and Yang Yang. "Achieving high efficiency white polymer light emitting device" *Adv. Mater.* **18**, 114 (2006)
4. V. Shrotriya, E. H. Wu, G. Li, Y. Yao and Y. Yang. "Efficient light harvesting in multiple-device stacked structure for polymer solar cells", *Applied Physics Letters*. **88**, 064104 (2006).
5. V. Shrotriya, G. Li, Y. Yao, C.-W. Chu and Y. Yang. "Transition metal oxides as buffer layer for polymer photovoltaic devices" *Applied Physics Letters*, **88**, 073508 (2006).
6. W. Chu, S. H. Li, C. W. Chen, V. Shrotriya, and Y. Yang, "High-performance organic thin-film transistors with metal oxide/metal bilayer electrode" *Appl. Phys. Lett.* **87**, 193508 (2005).
7. G. Li, V. Shrotriya, J. Huang, Y. Yao, T. Moriarty, K. Emery and Y. Yang, "High efficiency solution processable polymer photovoltaic cells by self organization of polymer blends," *Nature Materials* **4**, 864 (2005).
8. C.-W. Chu, J. Ouyang, J.-H. Tseng and Y. Yang, "Organic donor-acceptor system exhibiting electrical bistability for use in memory devices," *Adv. Mater.* **17**, 1440 (2005).
9. G. Li, V. Shrotriya, Y. Yao and Y. Yang. "Investigation of annealing effects and film thickness dependence of polymer solar cells based on poly(3-hexylthiophene)" *Journal of Applied Physics* **98**, 043704 (2005).
10. V. Shrotriya, J. Ouyang, Ricky J. Tseng, G. Li and Y. Yang. "Absorption spectra modification in poly(3-hexylthiophene):methanofullerene blend thin films", *Chemical Physics Letters* **411**, 138 (2005).
11. V. Shrotriya and Y. Yang. "Capacitance-voltage characterization of polymer light emitting diodes" *Journal of Applied Physics* **97**, 054504 (2005).

12. C.-W. Chu, Y. Shao, V. Shrotriya and Y. Yang. "Efficient photovoltaic energy conversion in tetracene-C₆₀ based heterojunctions" *Applied Physics Letters* **86**, 243506 (2005).
13. Liping Ma, Qianfei Xu, and Yang Yang, "Organic nonvolatile memory by controlling the dynamic copper-ion concentration within the organic layer" *Appl. Phys. Lett.* **84**, 4908(2004).
14. Liping Ma, Jianyong Ouyang, and Yang Yang, "High-speed and high-current density C₆₀ diodes" *Appl. Phys. Lett.* **84**, 4908(2004)
15. Jianhua Wu, Liping Ma, Yang Yang, "Single-band Hubbard model for the transport properties in bistable organic/metal nanoclusters/organic devices" *Phys. Rev. B* **69**, 11531(2004).
16. Fang-chung Chen, Qianfei Xu, and Yang Yang, "High performance polymer photovoltaic cells", *Appl. Phys. Lett.* **84**, 3181, (2004).
17. Fang-Chung Chen, Chih-Wei Chu, Jun He, Yang Yang, and Jen-Lien Lin, "Organic thin-film transistors with nanocomposite dielectric gate insulator" *Appl. Phys. Lett.* **85**, 11 (2004)

Interactions/Transitions

1. Presentations at meetings

1. "Polymer Materials for Microelectronics and Photonics" Maui Westin Hotel in Hawaii from December 11 to 14, 2005. Title "Polymer/nano particle composite for high performance electronic devices".
2. 2nd International Workshop on Polymer/Metal Nanocomposites, 2005, Institute of Chemistry, GKSS Research Centre, Geesthacht, Germany, Polymer/Metal Nanocomposites as the next generation electronic digital

memory devices". Sept. 26-27, 2005.

3. 30th memorial conference of Japan society for the Promotion of Science, Chitose, Hokkaido, Japan, Sept 2 and 3rd. High performance polymer electronic devices - solar cells, memories, and LEDs
4. 2005 Gordon Research Conference on the Chemistry of Electronic Materials, Connecticut College in New London, CT, 17 July to 22 July, 2005. High performance organic electronic devices: memory, solar cells, and LEDs.
5. The Physics and Chemistry of Switching in Condensed Matter Workshop, April 1 & 2, 2005, San Francisco, CA, USA. "Organic and polymeric nonvolatile memory devices"
6. The 5th International Conference on Electroluminescence of Molecular Materials and Related Phenomena, Jan. 17 – 21, Phoenix Az., Organic Thin Film Switching and Memory Devices.
7. MRS Fall Meeting, December 28th – Dec. 3rd, 2004, Boston, "Organic thin film nonvolatile memory", December 2nd, 2004.
8. Chemistry Department, University of Pennsylvania. Oct. 16th, 2004. Organic memory devices.
9. ICSM 2004, June 28th – July 2nd 2004, Wollongong, Australia, "High performance organic/polymeric memory devices",
10. Materials Research Society Spring Meeting, April 12th – 16th, 2004, San Francisco, California; "Toward all organic component circuits-from diodes to memory devices".
11. Asia Society of Information Display, "Ultra-high efficiency polymer light-emitting diodes". February 2004, Naging, China.
12. Sukant Tripathy Memorial Symposium, December 5th, Lowell Massachusetts, "Recent progress on organic electronics." (2003)
13. Materials Research Society Fall Meeting, December 1st -5th, 2003, Boston, Massachusetts; "High Performance Organic Memory Devices".
14. IBM Almaden Research Center, Colloquium, "High performance organic bistable and memory devices", November 14th, 2003.
15. The 6th Symposium on Electronic Processes in Organic Solids, Molecular Opto-electronic Materials, and related Phenomena", October 16th- 21st, 2003, Wuhan, China. Title: "Recent progress in flexible electronics at UCLA".
16. Rochester University, Department of Colloquium Physics Department, "High performance organic bistable and memory devices"
17. Cornell University, Department of Materials Science and Engineering, September 25, 2003, "High performance organic bistable and memory devices".
18. Organic Light-Emitting Device Workshop 2003, September 1-3, 2003 Hong Kong. Title: "Polymer morphology and the performance of polymer LEDs".
19. International Conference on Electroluminescence 4, Sept. 26-29, 2003, Cheju Island, Korea. Title: "Organic alloy and the formation of organic LEDs"

20. Dow Corning Company Colloquium, Midland, May 4th, 2003. Title: Recent progress on flexible electronics.
21. Material Research Society Spring Meeting, San Francisco, April, 2003. Title: Organic bistable and memory device”
22. Second International Conference on Molecular Electronics and Bioelectronics (M&BE2), Tokyo, Japan, March 5-7, 2003. Title” Organic/metal interface formation and interface engineering”
23. International Display Manufacture Conference, Feb. 18-21, 2003, Taipei, Taiwan. Title” Polymer LEDs and their recent progress”.

2. Transitions

1. Polymer memory patent has been licensed by Rohm and Haas.
2. Solar Cell Patent is under negotiation with several companies.
3. White polymer light emitting diodes patent is also under negotiation with several companies.

New Discoveries, Inventions, or Patent disclosures:

We have several important discoveries and patents applied that supported by AFOSR, The high-speed organic diode, the organic memory from nano-interface engineering, and the high-current output and low working voltage organic thin film transistor as follows,

1. Yang Yang and Liping Ma, Vertical Organic Field Effect Transistor filed 2004, provisional -- UCLA2004-074-2, licensed by ORFID Corporation).
2. Yang Yang and Liping Ma, Novel organic electrical bistable device from nano-interface engineering (2004).
3. Organic-Complex Thin Film with Electrical Bistability. (2005)
4. Stacked Layer Electrode for Organic Electronic Devices. (2005)
5. Highly Efficient Photovoltaic Cells Prepared by Self-Organization of Polymer Composite. (2005)

Honors/Awards:

1. Outstanding Overseas Chinese Scientist, Natural Science Foundation-China, (2004)
2. Outstanding Alumni Award, U-Mass Lowell, (1999)
3. NSF Career Award, (1998);
4. 3M Young Investigator Award, (1998);

Research Details (Part I)

High performance vertical organic transistor

1. Introduction

Organic field effect transistors (OFETs) have attracted considerable attention since their discovery^{1,2} due to their flexibility, low cost, and amenability to fabrication over large surface areas.^{3,4} However, the performance of OFETs are still poor compared to their inorganic counterparts, showing low current output (on the order of μA) and high working voltages (up to 100 V) in general.^{4,5} High current output and low working voltage OFETs are highly desired for many applications such as active-matrix flat panel displays,⁶ such as switching of organic light-emitting diodes (OLEDs). Several approaches to enhance the OFETs' performance, such as decreasing the channel length and increasing the dielectric constant of the gate dielectrics, have been reported.^{7,8,11-15} Decreasing the channel length can be realized by lithography techniques and vertical architectures.¹²⁻¹⁵ Conventional vertical transistors do not intrinsically increase the cross sectional area, which limits their current output.

2. Results and Discussion

(1) Proposed device structure

Fig. 1(a) shows a schematic diagram of the device structure. It consists of an active cell on top of a capacitor cell. The top electrode and the bottom electrode are

defined as the drain and gate electrode, respectively. This device is defined as a gate-source-drain vertical organic field-effect transistor (VOFET).

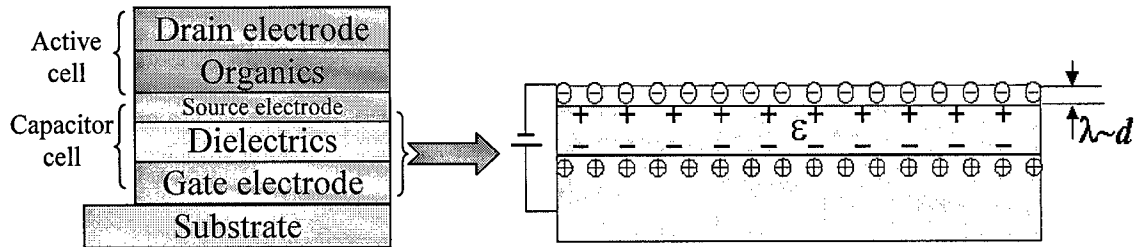


Fig. 1 (a) The schematic diagram of the device structure. The transistor consists of an active cell and a capacitor cell. This device is quite different from traditional FETs which the gate is always between the source and drain.

Fig. 1(b) The mechanism of our FET is still not clear yet, however, it is believed this device is due to a nanometer-scale phenomenon, so-called "Near-Field Effect". When the charge distribution length (λ) is comparable with the thickness (d) of the source electrode layer, an electric field exists at the organic/source interface, which modifies the source-drain current.

(2) Proposed device operation principle

The transistor operates in the following fashion. An n-type organic semiconductor is used for the active cell. The source electrode is used as a common cathode for both the capacitor cell and the active cell. Consequently, the current injection for the active cell is controlled by electron injection from the source electrode. The materials with mismatched energy levels between the organic semiconductor and the

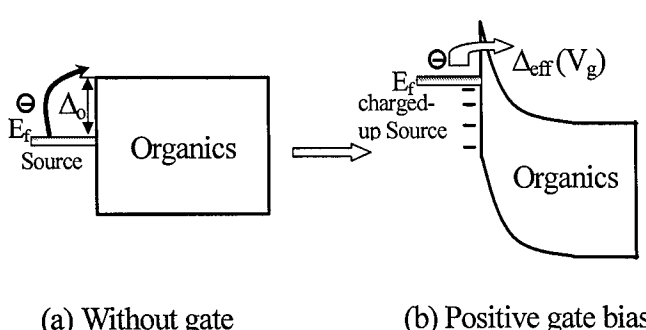


Fig. 2. The schematic band diagram for the VOFET which demonstrates its operating principles: (a) without bias, and (b) with positive gate bias.

source electrode at zero gate-bias condition were selected in order to achieve low leakage current. This approach is similar to that of a Schottky barrier transistor.¹⁶ Special attention

is paid to the interface between the source electrode and the organic semiconductor layer to demonstrate the device working principle (Fig. 2). Before applying a gate bias (Fig. 2(a)), the large injection barrier height (Δ_0) (due to the energy level mismatch described above) prevents electron injection efficiently from the source electrode into the semiconductor layer. When the gate is positively biased (Fig. 2(b)), the capacitor cell is charged up. Negative charge is then built-up within the source electrode layer. As a result, the electron injection barrier height from the source into the organic layer is lowered by an amount (δ). Hence, the effective energy barrier height (Δ_{eff}) for electron injection from the source electrode is decreased ($\Delta_{\text{eff}} = \Delta_0 - \delta$), allowing efficient electron injection from the source into the semiconductor layer causing an increase of the source-drain current (I_{sd}) when a drain bias is applied. At a constant drain-source bias (V_{ds}) and temperature (T), the gate potential (V_g) controls the stored charge in the capacitor cell and the δ term. Therefore, V_g controls the effective energy barrier height, $\Delta_{\text{eff}}(V_g) = \Delta_0 - \delta(V_g)$. Taking the temperature and applied drain bias as constant, it is reasonable to assume that the injection current has an exponential relation with the effective energy barrier, $I(V_g) = I_0 \cdot \exp[-\Delta_{\text{eff}}(V_g) / (kT)]$, where k is Boltzmann constant, I_0 is a constant.¹⁷

(3) I-V characteristics and On/Off ratio

Drain-source I-V characteristics at various gate potentials for a VOFET with

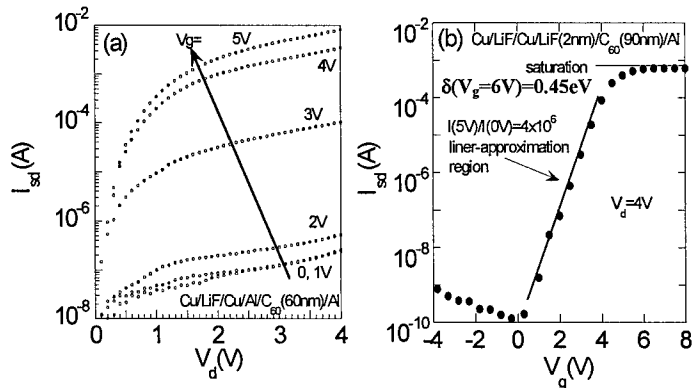


Fig. 3. (a) The I_{sd} - V_d characteristics of a VOFET at various gate biases. (b) The I_{sd} - V_g characteristics at $V_d = 4$ V for a VOFET with LiF buffer layer at the source/ C_{60} interface.

C_{60} as the organic layer and Cu/Al as the source electrode are shown in Fig. 3(a). For this device the current output is near 10 mA (or 4 A/cm^2) at working voltage less than 5 V. It should be mentioned that the leakage current from gate to source is in the μA range. The ON/OFF ratio (current ratio at certain drain voltage with and without gate bias) at 5 V gate bias and 4 V drain bias is near 10^5 . In order to further increase the ON/OFF ratio, a 2nm-thick LiF layer was put between the source and organic contact and it was found that the OFF-state current was much reduced. It can be seen from Fig. 3 (b) that at 4V drain bias the $\text{ON}(V_g = 5 \text{ V})/\text{OFF}(V_g = 0 \text{ V})$ ratio for the device is 4×10^6 . It should be noted that the current output for the device with the LiF buffer layer is not as high as the previous device. One possible reason is that the C_{60} layer is thicker in this device than in the previous one (90 nm vs. 60 nm) which limits the current. Fine tuning the device structure, materials, thickness, and fabrication conditions may further enhance the device performance.

C_{60} is an n-type semiconductor which was selected as the organic material. The origin of the injection barrier, shown in Fig. 2, is caused by the mismatch of the metal Fermi level with the C_{60} conductance band, so that electrons are transported through an injection barrier from the source electrode to the C_{60} layer.¹⁸ To explain the functional dependence of I_{sd} on V_g in Fig. 4(b), the effective barrier can be mathematically expanded as $\Delta_{\text{eff}}(V_g) = \Delta_0 - \alpha V_g - \beta V_g^2 - \dots$, where Δ_0 and α, β are constants. It was found for some regions, a liner approximation, $\delta(V_g) = \alpha V_g$, can describe well the I_{sd} - V_g characteristics for some of the devices, where $I_{ds}(V_g) = I_0 * \exp(\alpha V_g / (kT))$. Using this equation the exponential increase of the I_{sd} with the increase of the gate potential within a certain range can be explained. As the gate potential increases, the effective barrier

height Δ_{eff} decreases. It is found that for the data shown in Fig. 2(b) the $\delta(V_g=6\text{V})$ is about 0.45 eV. One can imagine that above a certain gate voltage Δ_{eff} may reach zero, and the electrons have no injection barrier into the organic layer. In this case, the source-drain current is changed from injection-controlled to the bulk-controlled, and a saturation shows up in $I_{\text{sd}}\text{-}V_g$.

3. Conclusion

A stacked-structure field effect transistor with an active cell on top of a capacitor cell was demonstrated. High-capacitance capacitor cell and very thin and rough source electrode layer are important for device operation. Organic transistors with low working voltage (less than 5 V), high current output (up to 10 mA or 4 A/cm^2), and high ON/OFF ratio (4×10^6) was obtained. The transistors can be incorporated with other organic electronic devices such as organic light-emitting diodes. This novel device with its enhanced operating characteristics opens new directions in basic scientific research for organic transistors and their applications.

References:

1. F. Ebisawa, T. Kurokawa, and S. Nara, *J. Appl. Phys.* **54**, 3255(1983).
2. A. Tsumura, H. Koezuka, and T. Ando, *Appl. Phys. Lett.* **49**, 1210(1986).
3. G. Horowitz, *Adv. Mater.* **10**, 365(1998).
4. C.D. Dimitrakopoulos and P.R.L. Malenfant, *Adv. Mater.* **14**, 99(2002).
5. G. Wang, Y. Luo, and P.H. Beton, *Appl. Phys. Lett.* **83**, 3108(2003).
6. A. Dodabalapur, Z. Bao, A. Makhija, J.G. Laquindanum, V.R. Raju, Y. Feng, H.E. Katz, and J. Rogers, *Appl. Phys. Lett.* **73**, 142(1998).
7. F. Garnier, R. Hajlaoui, and M. E. Kassmi, *Appl. Phys. Lett.* **73**, 1721, (1998).
8. C.D. Dimitrakopoulos, S. Purushothaman, J. Kymissis, A. Callegari, and J. M. Shaw, *Science* **283**, 822 (1999).
9. G. Velu, C. Legrand, O. Tharaud, A. Chapoton, D. Remiens, and G. Horowitz, *Appl. Phys. Lett.* **79**, 659, (2001).
10. G. D. Wilk, R. M. Wallace, and J. M. Anthony, *J. Appl. Phys.* **89**, 5243, (2001).
11. G.M. Wang, D. Moses, A.J. Heeger, H.M. Zhang, M. Narasimhan, R.E. Demaray, *J. Appl. Phys.* **95**, 316(2004).

12. Y.J. Zhang, J.R. Pena, S. Ambily, Y.L. Shen, D.C. Ralph, G.G. Malliaras, *Adv. Materials* **15**, 1632(2003).
13. Y. Yang, A.J. Heeger, *Nature* **372**, 344(1994).
14. N. Stutzmann, R.F. Friend, H. Sirringhaus, *Science* **299**, 1881(2003).
15. R. Parashkov, E. Becker, S. Hartmann, G. Ginev, D. Schneider, H. Krautwald, T. Dobbertin, D. Metzdorf, F. Brunetti, Schildknecht, A. Kammoun, M. Brandes, T. Riedl, H. Johannes, and W. Kowalsky, *Appl. Phys. Lett.* **82**, 4579(2003).
16. S. Heinze, J. Tersoff, R. Martel, V. Derycke, J. Appenzeller, and Ph. Avouris, *Phys. Rev. Lett.* **89**, 106801-1(2002).
17. J.C. Scott, *J. Vac. Sci. Technol. A* **21**, 521(2003).
18. L. P. Ma, J. Y. Ouyang, and Y. Yang, *Appl. Phys. Lett.*, **84**, 4908(2004).

Research Details (Part II)

High efficiency polymer bulk-heterojunction solar cells by self-organization

1. Introduction

Polymer solar cells have recently evolved as the promising cost effective alternatives to the silicon based solar cells.¹⁻³ Some of the important advantages of these so called “plastic” solar cells include low cost of fabrication, ease of processing, mechanical flexibility and versatility of chemical structure from advances in organic chemistry. However, low efficiency⁴⁻⁶ of these plastic solar cells limits their feasibility for commercial use. The efficiencies of polymer photovoltaic (PV) cells got a major boost with the introduction of bulk heterojunction (BHJ) concept^{7,8} consisting of an interpenetrating network of electron donor and acceptor materials. This concept has recently been demonstrated in small-molecular organic photovoltaics as well.⁹ It is argued that due to the space charge effects inherent in the BHJ structure, the fill factor is usually low and the disordered structure will be ultimately limited by high series resistance.¹⁰ To achieve highly efficient PV device, solar radiation needs to be efficiently absorbed, for

which the device thickness needs to be increased. However, this will further increase the series resistance of the device. Here we demonstrate that the series resistance of the polymer BHJ PV cells can be significantly reduced by polymer self-organization (to values as low as $1.56 \Omega \text{cm}^2$) by controlling the growth rate of the active polymer layer from solution to solid-state. The fill factor also increased to a value of more than 67 %, which is amongst the highest values reported for polymer solar cells. As a result, we achieved device power conversion efficiency of 4.4% under standard AM1.5G 1 Sun test condition. The PV cells fabricated in this study are made by solution-process, and large device area can be achieved by this process at relatively low cost.

2. Results and Discussion

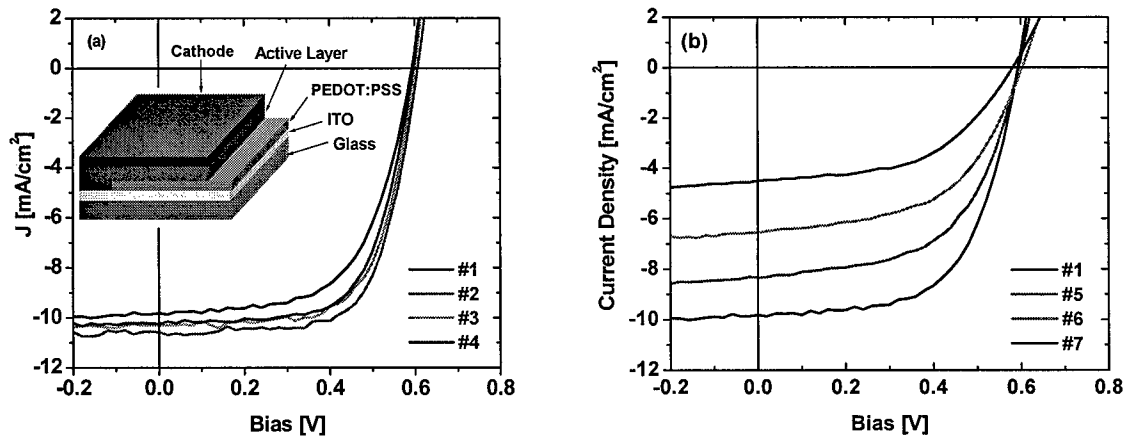


Figure 1: (a) The different J - V curves correspond to the devices with active layer before (#1), and after thermal annealing at 110°C for 10 min (#2), 20 min (#3), and 30 min (#4). (b) J - V characteristics under illumination for devices with different film growth rates by varying the solvent evaporation time, t_{evp} . The t_{evp} for different films were: 20 min (#1), 3 min (#5), 40 sec (#6), and 20 sec (#7).

The polymer PV device in this study consisted of an active layer of poly(3-hexylthiophene): [6,6]-phenyl- C_{61} -butyric acid methyl ester (P3HT:PCBM) sandwiched between metallic electrodes. The active layer was obtained by spin-coating the blend at

600 rpm for 60s, and the thickness of film was \sim 210-230 nm, as measured from Dektek profilometer. The active device area was 0.11 cm^2 . The growth rate of the polymer layer was controlled by varying the film solidification time. The films were wet after spin-coating and were then dried in covered glass petri dishes. Before cathode deposition, the films were thermally annealed at 110°C for various times. Testing was done in N_2 under simulated AM1.5G irradiation (100 mW/cm^2) using xenon-lamp based solar simulator (Oriel 96000 150W Solar Simulator). The current-voltage (J - V) curves under illumination for four devices with annealing times (t_A) of 0 (Device #1), 10 (#2), 20 (#3), and 30 min (#4) are shown in Figure 1(a). The annealing was performed at 110°C . Upon annealing, the short-circuit current (J_{SC}) increases slightly from 9.9 to 10.6 mA/cm^2 and the fill factor (FF) increases from 60.3% to 67.4%, which is amongst the highest FF in organic solar cells. As a result, the power conversion efficiency (PCE) improves from 3.5% to 4.4%.

The highly regular chain structure of poly(3-alkylthiophene)s (P3ATs) facilitates their self-organization into two-dimensional sheets via inter-chain stacking.¹¹ The slow growth will assist the formation of self-organized ordered structure in the P3HT:PCBM blend system. The degree of self-organization can be varied by controlling the film growth rate, or in other words, by controlling the time it takes for the wet films to solidify. In Figure 1(b) we compare the J - V characteristics of four devices with different solvent evaporation times (t_{evp}) after spin coating, judging by visual inspection of the change in film color when it solidifies from the liquid phase. Device #1 was covered in glass petri dish while drying and had $t_{\text{evp}} \sim 20$ min, #5 was left open in N_2 ambient and had $t_{\text{evp}} \sim 3$ min, #6 and #7 were dried by putting on hot plate at 50°C and 70°C , respectively, and

had $t_{\text{evp}} \sim 40$ s and ~ 20 s. The J_{SC} reduces from 9.9 to 8.3, 6.6, and 4.5 mA/cm², and the device series resistance, R_{SA} , increases from 2.4 to 4.5, 12.5, and, 19.8 Ω.cm² with reducing t_{evp} . The FF also consistently decreases from 60.3% to 52.0%. Figure 2 shows the results of external quantum efficiency (EQE) measurements for two types of devices, slow grown (#1) and fast grown (#7). The EQE for device with fast grown film shows a maximum of $\sim 19\%$ at a wavelength of 350 nm. On the other hand, for the device with slow grown film, the EQE maximum increases by more than three times to $\sim 63\%$ at 500 nm. The integral of the product of this absolute EQE and the global reference spectrum yields a J_{SC} of 9.47 mA/cm² which matches closely to the J_{SC} that we measured for this particular device. This increase in quantum efficiency over the wavelength range of 350-650 nm contributes to the increase in the power conversion efficiency of our devices. We believe that this enhancement in EQE originates from two important contributions, an increase in the charge carrier mobility, and increased absorption in the active layer. The discussion on the effect of slow growth rate on the charge carrier mobility and the absorption spectra of the films follows.

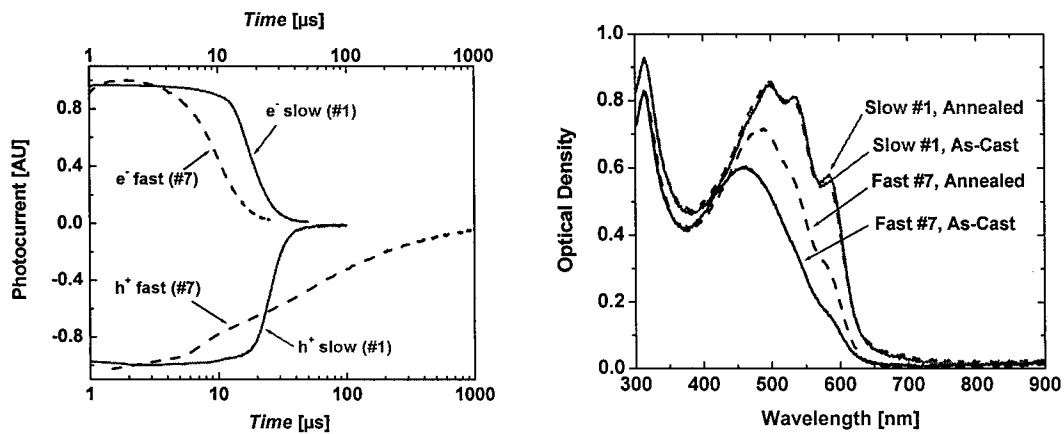


Figure 4. UV-Vis absorption spectra for films of P3HT:PCBM (in 1:1 wt. ratio), for both slow (#1) and fast (#7) grown films before and after thermal annealing

TOF study was conducted on slow (#1) and fast (#7) grown films at $E \sim 2 \times 10^5$ V/cm. The film preparation method for TOF measurements was the same as that for device fabrication to maintain maximum similarity for reliable comparison. As clearly seen in Figure 3, in the film prepared with conditions similar to device #1 (or the slow grown film), both electron and hole transport non-dispersively with $\mu_e = 7.7 \times 10^{-5}$ and $\mu_h = 5.1 \times 10^{-5}$ cm²/V-s, whereas for film #7, fast growth leads to dispersive hole transport and significant reduction in μ_h to 5.1×10^{-6} cm²/V-s. The electron mobility increases slightly to 1.1×10^{-4} cm²/V-s. The destruction of ordered structure during fast growth is believed to be the reason. For the slow grown film, the hole mobility is similar to (or slightly higher than) the values reported earlier for poly(p-phenylenevinylene):PCBM blends^{12,13}, and the ratio between electron and hole mobilities is close to unity ($\mu_e/\mu_h \sim 1.5$) resulting in balanced carrier transport in the active layer. This results in FF values of more than 67% for the best devices. The measured optical densities for slow (#1) and fast (#7) grown films are shown in Figure 4, before and after thermal annealing at 110°C for 20 min. Compared to the film dried at 70°C (#7), the absorption in red region of the slow grown film (#1) is much stronger. The three vibronic absorption shoulders (peaks) are much more pronounced in film #1, indicating higher degree of ordering.¹⁴ After annealing at 110°C for 20 min, the absorbance of film #7 shows significant increment and the vibronic features become clearer, indicating a partial recovery of ordering. During the fast growth of the film, the orientation of P3HT supermolecules is forced by the short time scale and is not thermodynamically stable.

3. Conclusion

In conclusion, we have fabricated polymer photovoltaic cells utilizing thick active layer with power conversion efficiency of 4.4%. The self-organization of polymer chains during the slow film growth from liquid phase, enhanced light absorption due to the film thickness, and the rough interface are believed to be mainly responsible for the high device efficiency. The efficiency value reported here is the highest ever reported for polymer BHJ PV cells to the best of our knowledge. The results will help in better understanding the underlying relationship between the polymer morphology and the device performance, and will subsequently help in enhancing the efficiencies of plastic solar cells to a level of practical applications.

References

1. Brabec, C. J., Sariciftci, N. S. & Hummelen, J. C. Plastic solar cells. *Adv. Funct. Mater.* **11**, 15-26 (2001).
2. Coakley, K. M. & McGehee, M. D. Conjugated polymer photovoltaic cells. *Chem. Mater.* **16**, 4533-4542 (2004).
3. Brabec, C. J. Organic photovoltaics: technology and market. *Solar Energy Mater. & Solar Cells* **83**, 273-292 (2004).
4. Shaheen, S. E. et al. 2.5% efficient organic plastic solar cells. *Appl. Phys. Lett.* **78**, 841-843 (2001).
5. Padinger, F., Rittberger, R. S. & Sariciftci, N. S. Effects of post production treatment on plastic solar cells. *Adv. Funct. Mater.* **13**, 85-88 (2003).
6. Walduf, C., Schilinsky, P., Hauch, J. & Brabec, C. J. Material and device concepts for organic photovoltaics: towards competitive efficiencies. *Thin Solid Films* **451-452**, 503-507 (2004).
7. Yu, G., Gao, J., Hummelen, J. C., Wudl, F. & Heeger, A. J. Polymer photovoltaic cells: enhanced efficiencies via a network of internal donor-acceptor heterojunctions. *Science* **270**, 1789-1791 (1995).
8. Saraciftci, N. S., Smilowitz, L., Heeger, A. J. & Wudl, F. Photoinduced electron transfer from a conducting polymer to buckminsterfullerene. *Science* **258**, 1474-1476 (1992).
9. Peumans, P., Uchida, S. & Forrest, S. R. Efficient bulk-heterojunction photovoltaic cells using small-molecular-weight organic thin films. *Nature* **425**, 158-162 (2003).
10. Yang, F., Shtein, M. & Forrest, S. R. Controlled growth of a molecular bulk heterojunction photovoltaic cell, *Nature Materials* **4**, 37-41 (2005).

11. Grevin, B., Rannou, P., Payerne, R., Pron, A. & Travers, J. P. Multi-scale scanning tunneling microscopy imaging of self-organized regioregular poly(3-hexylthiophene) films. *J. Chem. Phys.* **118**, 7097-7102 (2003).
12. Choulis S. A. et al. Investigation of transport properties in polymer/fullerene blends using time-of-flight photocurrent measurements. *Appl. Phys. Lett.* **83**, 3812-3814 (2003).
13. Mihailetti, V. D. et al. Compositional dependence of the performance of poly(p-phenylenevinylene):methanofullerene bulk-heterojunction solar cells. *Adv. Funct. Mater.* **15**, 795-801 (2005).
14. Sunderberg, M., Inganäs, O., Stafstrom, S., Gustafsson, G. & Sjogren, B. Optical absorption of poly(3-alkylthiophenes) at low temperatures. *Solid State Communications* **71**, 435-439 (1989).

Research Details (Part III)

New Materials for High Efficient Blue Organic Light-emitting Diodes

1. Introduction

Silicon semiconductor technology has driven the profusion of information technology into every aspect of modern life. An obvious example of this is the emergence of portable electronic devices that are rapidly becoming essential; cell phones, personal digital assistants, palmtop computers, etc. These share a common Achilles heel, namely, battery life. The most obvious way to attack this problem is through replacement of the power hungry back-lit LCD displays that reside in all light weight devices. It is this impetus that has brought organic light emitting devices (OLEDs) to the forefront of modern materials science. The ability to mass produce thin, efficient, bright displays from organic polymers and small molecules (PLEDs and OLEDs respectively) that can supplant modern LCDs depends almost entirely on the ability to

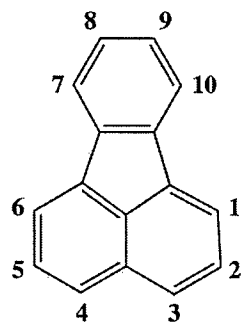


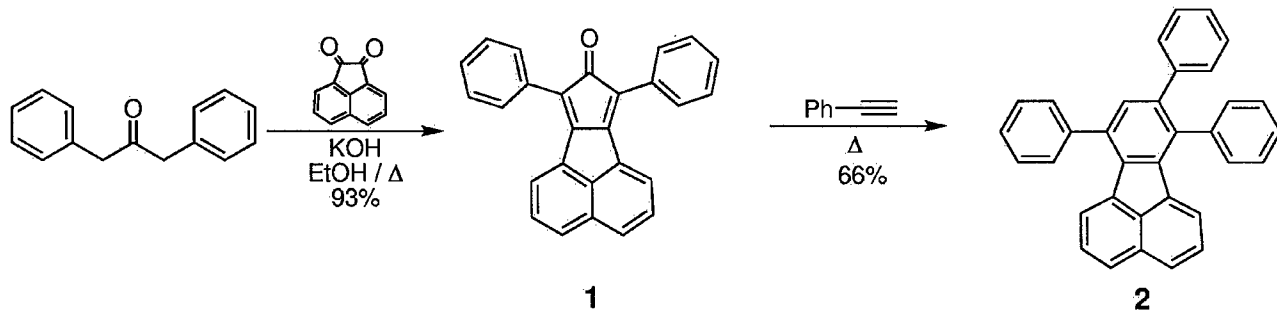
Figure 1 Fluoranthene with relevant carbons numbered

create new materials that can undergo efficient electroluminescence at a variety of wavelengths. This has lead to many publications and patents but to date has failed to produce an efficient, cheap, and robust blue-emitter. It is, of course, not an easy task to find a small molecule that possesses, not only a very large band gap, but stability to the harsh electrochemical environment of OLEDs and a very large quantum yield in the solid state. One class of molecules in particular, fluorenes – especially spiro-fluorenes^[1] – has received much attention because of the outstanding properties in this area,^[2-3] but lengthy syntheses and low-yielding steps such as boronic acid/ester formations are less than ideal for single layer/host materials. In an effort to redirect some of the explorations, we have investigated a close cousin of fluorenes – fluoranthenes – for applications as blue-emitters in OLEDs (Figure 1). In particular, 7,8,10-triphenylfluoranthene (TPF), a highly luminescent solid-state blue-emitting small molecule that can be obtained in two steps from commercial starting materials.

2. Results and Discussion

After the elucidation of the structure of fluoranthene at the turn of the 20th century, the chemistry of fluoranthenes evolved rapidly.^[4] Studies of the interesting photophysical properties,^[5-6] followed but interest in fluoranthenes faded fast. Of particular note is the synthesis of fluoranthene derivatives by a double Knoevenagel condensation between a 2-propanone and acenaphthenequinone which allows functionalization at the 7 and 10 positions.^[7] A subsequent Diels-Alder addition allows further functionalization at the 8 and 9 positions.^[7-8] Finally, starting from bromoacenaphthenequinone,^[9] the 3 position is open to functionalization. With these synthetic tools in hand we set about finding a fluoranthene derivative that would not

crystallize and remained highly blue-luminescent in the solid state. The most obvious candidate was a perphenylated derivative which, due to steric hindrance would keep the phenyl rings out of plane, thus presenting a ball-like surface to resist crystallization and reduce facial contacts that can lead to excimer quenching and bathochromic shifts in emission. To our surprise only the 7,8,10-triphenyl derivative (**2**) exhibited strong luminescence, the 7,8,9,10-tetraphenyl derivative is essentially non-fluorescent (in the solid state) and the 3,7,8,9-tetraphenyl derivative suffers from a large bathochromic shift in the solid state. The introduction of other functionality (e.g. esters, carboxylic acids, and halides) led to green/yellow emission and/or solubility problems. As with the other derivatives, 7,8,10-triphenylfluoranthene (TPF) was synthesized via the Knoevenagel/Diels-Alder method from acenapthenequinone, diphenylacetone, and phenylacetylene, using only ethanol and (optionally) xylenes for solvents; all are inexpensive and readily available (Scheme 1). Purification is uncomplicated and can be accomplished by precipitation from ethanol/benzene, flash chromatography, sublimation,



Scheme 1 The synthesis of 7,8,10-triphenylfluoranthene.
or any combination of these.

Unsubstituted fluoranthene is known to form very stable anions that are long-lived enough to dimerize.^[10] Although dimerization is prevented by the three phenyl substituents in TPF, it retains a stable reversible reduction (Figure 2). Unfortunately the

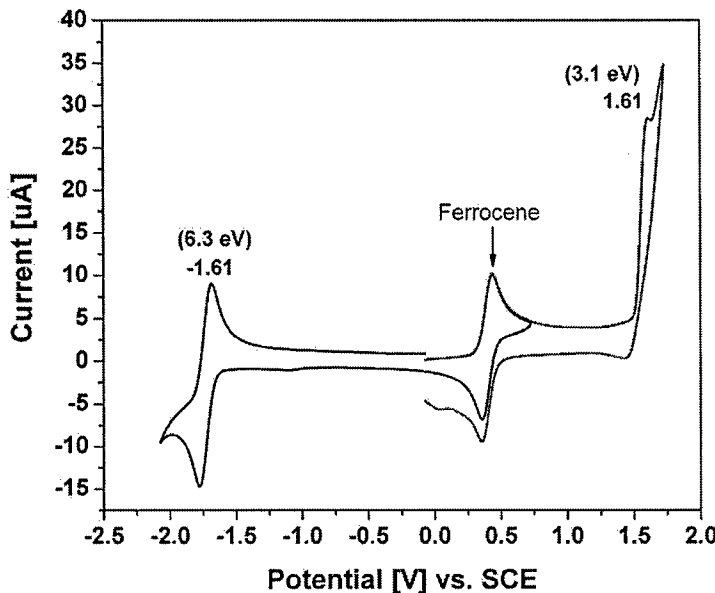


Figure 2 Cyclic voltammogram of TPF in $\text{CH}_3\text{CN}/10^{-1} \text{ M Bu}_4\text{NPF}_6$. The numbers above represent peak values with the parenthetical numbers representing absolute HOMO/LUMO energies.

same stability is not observed in the oxidation wave by solution phase CV. The absence of a cogent decomposition pathway for TPF (e.g. via fragmentation or gas evolution) implies the existence of a radical-cation (or oxidized species) that reacts with the solvent or supporting electrolyte^[11] and does not necessarily translate into reduced device performance or lifetime due to oxidative decomposition. Owing to the close proximity of the phenyl substituents, the irreversibility may also be due to an intramolecular cyclodehydrogenation of close phenyl substituents. While we were able to prepare the cyclodehydrogenated product chemically, we saw no evidence of its formation by spectroelectrochemical measurements. Despite the imposition of an irreversible

oxidation wave, the introduction of three phenyl groups does not significantly change the REDOX potentials (or HOMO/LUMO gap) from that of fluoranthene with: $E_p^a = 1.61$ V, $E_{1/2}^c = -1.72$ V vs SCE for TPF and $E_p^a = 1.617$ V, $E_{1/2}^c = -1.81$ V vs. SCE for fluoranthene.

The most promising properties of TPF for device applications are the apparent resistance to solid-state quenching / excimer emission and stability (decomposition was not observed by TGA due to sublimation at *ca.* 300 °C without the observation of mass loss below that temperature). As demonstrated by benzo[*k*]fluoranthene, which has a quantum yield of 1, the quantum yield of TPF is not the highest of the fluoranthenes. Benzo[*k*]fluoranthene, however, is completely quenched in the solid state, which is not true of fluoranthene or TPF. Relative quantum yield measurements of TPF revealed a solvent dependence, with $\Phi_{rel} = 0.38$ in CH_2Cl_2 and $\Phi_{rel} = 0.52$ in cyclohexane; this is not uncommon. More importantly, though, are the solid-state quantum yield measurements of TPF films (using an integrating sphere) which reached as high as 0.86 for PMMA dispersions and were as low as 0.51 for pure TPF films. The high quantum yield in PMMA dispersions is probably due to the rigid matrix which further hinders rotation of the phenyl substituents and distortions in the fluoranthene core. The discrepancy between the pure TPF film and PMMA dispersion may be related to a quenching mechanism or, more likely, the poor suitability of TPF films cast from solvents for our integrating sphere apparatus which was much better suited for PMMA monoliths than thin films. Evaporated films were simply too thin to obtain a reasonable signal to noise ratio. The photoluminescence (PL) spectrum at 77 K exhibits three peaks at 423, 448 (λ_{max}), and 478 with a small Stokes shift (Figure 3). At room temperature, in solution

λ_{\max} shifts to 458 nm, and 468 nm in the solid state. Although TPF emits from the triplet

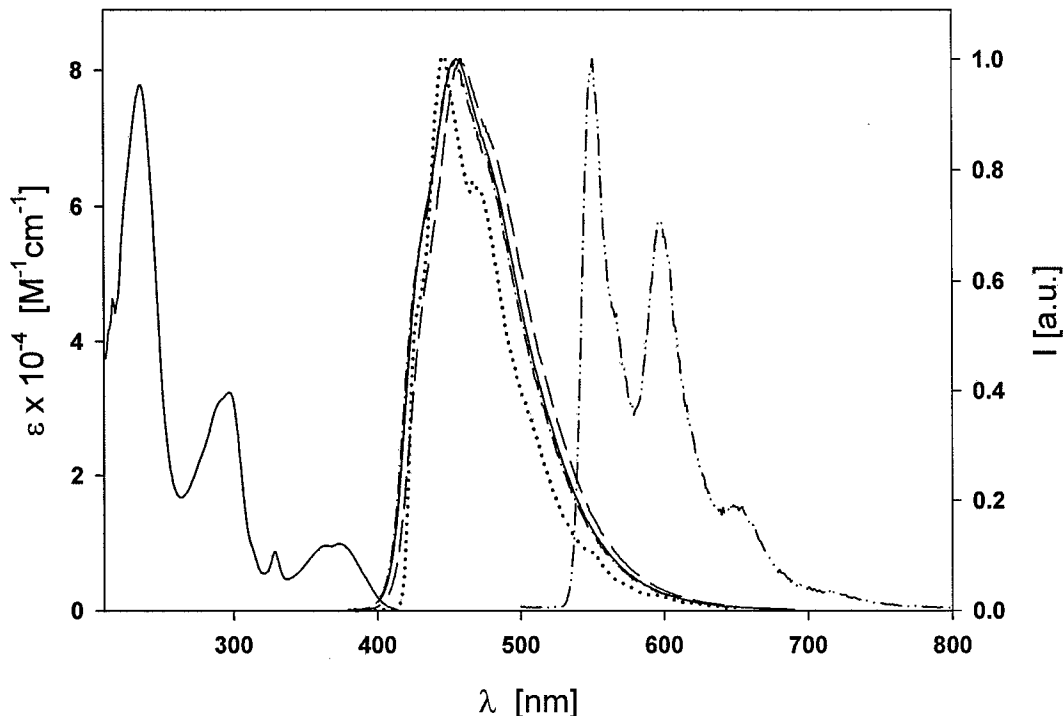


Figure 3 Absorption/normalized emission spectra of TPF; UV-Visible absorption (—); 77 K fluorescence (···); 298 K fluorescence in CH_2Cl_2 (—); solid-state fluorescence (—); 77 K phosphorescence (—···).

state, the reported phosphorescence spectrum is only attainable in a frozen glasse (at 77K) and is far less intense than any fluorescence bands; the signal was too weak for accurate lifetime measurements.

A typical blue OLED using TPF as a highly efficient blue emissive material is shown in Figure 4, where the inset shows the device structure. A second hole transporting layer (HTL) of 15 nm 4,4'-dicarbazolyl-1,1'-biphenyl (CBP) had to be inserted between the 4,4'-bis-(1-naphthyl-N-phenylamino)-biphenyl (NPB) and TPF to increase the device efficiency. The high homo energy of TPF (~6.3 eV, calculated from cyclic voltammetry) was better matched to CBP, which has a HOMO energy of 5.7 eV

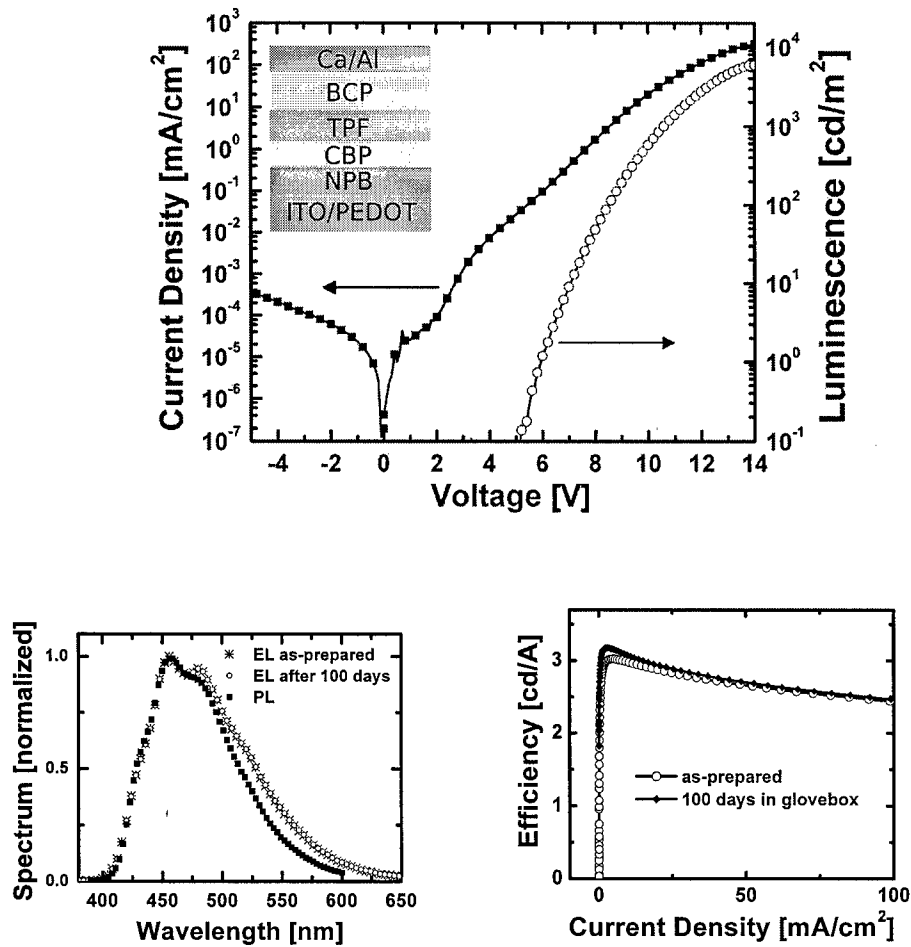


Figure 4 The electrical characteristics of a typical TPF-based OLED. (A) Current-voltage-luminescence characteristics (inset shows the device structure), (B) the electroluminescence spectra and (C) the electroluminescence efficiency, both for a pristine device and one that has been stored under nitrogen for 100 days.

and should more efficiently inject holes from HTL into the TPF layer.^[12] Figure 4(a) shows the current-voltage-luminescence (*I-V-L*) characteristics. Under reverse bias, charge injection is difficult and the leakage current is constant at 10^{-4} mA/cm².

The device current turns on at 2.3 V, which is the potential at which electron and hole injection from electrodes to the device begins. While the electrons and holes appear to reach the light-emitting layer, no light emission occurs below a voltage of 5 V. This 2.6 V difference between charge injection and light emission is accompanied by a small inflection in the I-V curve but the current does not abruptly increase or saturate in the high voltage region. This suggests that the electron and hole carriers are not well balanced, and a better-optimized device structure could further increase the efficiency. A

maximum luminescence of 5910 cd/m^2 occurs at 320 mA/cm^2 . The fine structure of the EL spectrum, with peaks at 456 nm (λ_{\max}) and 480 nm and CIE of $x = 0.177$, $y = 0.24$ (Figure 4(b)), is consistent with the PL spectra (Figure 3); this correlation is indicative of a common charge recombination and decay mechanism for EL and PL. There is a slight broadening in the EL spectrum, as compared to the solid-state PL spectrum, and more fine structure is present than in either solution or solid-state room temperature PL spectrum. The maximum efficiency reaches 3.02 cd/A ($1.83\% \Phi_{\text{external}}$) with a power efficiency of 1.1 lm/W at 4.93 mA/cm^2 (Figure 4(c)), which is comparable to other fluorescent blue-emitting hydrocarbons such as anthracene derivatives^[13-14] and spirobifluorenes,^[15] however, bright blue light emission is achieved with only a single emissive layer, which simplifies the device fabrication process. The overall efficiency may be further increased by doping suitable phosphorescent dopants, as the large bandgap of TPF should allow it to readily sensitize blue-green to red dopants.

3. Conclusion

Although fluroanthenes have been around for the better part of a century, they have, until now, been overlooked for OLED applications.^[16] Starting from cheap commercially available starting materials we have synthesized a simple fluoranthene hydrocarbon that emits blue light in a single-layer device architecture with very respectable efficiencies and low turn-on voltages. Although the CIE coordinates of this initial device preclude immediate commercial applications, the ease of synthesis and derivatization makes fluoranthenes a viable new platform for future investigation as simple organic fluorophores. With further studies into device optimization TPF may prove to be an excellent blue emitter or host material for future OLED display

applications.

References:

1. D. Katsis, Y.H. Geng, J.J. Ou, S.W. Culligan, A. Trajkovska, S.H. Chen, L.J. Rothberg *Chem. Mater.* **14**, 1332 (2002).
2. K-T. Wong, Y-Y. Chien, R-T. Chen, C-F. Wang, Y-T. Lin, H-H. Chiang, P-Y. Hsieh, C-C. Wu, C. H. Chou, Y. O. Su, G-H. Lee, S-M. Peng *J. Am. Chem. Soc.* **124**, 11576 (2002).
3. C-C. Wu, T-L. Liu, W-Y. Hung, Y-T. Lin, K-T. Wong, R-T. Chen, Y-M. Chen, Y-Y. Chien *J. Am. Chem. Soc.*, **125**, 3710 (2003).
4. H.S. Tucker, M. Whalley, *Chem. Rev.* **50**, 483 (1952).
5. I.B. Berlman, H.O. Wirth, O.J. Steingraber, *J. Am. Chem. Soc.*, **90**, 566 (1968).
6. H. Güsten, G. Heinrich, *J. Photochem.* **18**, 9 (1982).
7. C.F.H. Allen, J.A. Van Allan *J. Org. Chem.* **17**, 845 (1952).
8. M. Wehmeier, Wagner, M., K Müllen *Chem. Eur. J.*, **7**, 2197 (2001).
9. H. G. Rule, S. B. Thompson *J. Chem. Soc.*, 1761 (1937).
10. S Wawzonek, J. W. Fang *J. Am. Chem. Soc.* **68**, 2541 (1946).
11. For a recent example, the electrochemical oxidation of C₆₀; C. Bruno, I. Doubitski, M. Marcaccio, F. Paolucci, D. Paolucci, A. Zaopo *J. Am. Chem. Soc.* **125**, 15738 (2003).
12. Y. T. Tao, E. Balasubramaniam, A. Danel, P. Tomaszik, *Appl. Phys. Lett.* **77**, 933 (2000).
13. J. Shi, C. W. Tang, *Appl. Phys. Lett.* **80**, 3201 (2002).
14. Y. Li, M.K. Fung, Z. Xie, S-T. Lee, L-S. Hung, J. Shi *Adv. Mater.* **14**, 1317 (2002).
15. C. C. Wu, Y. T. Lin, K. T. Wong, R. T. Chen, Y. Y. Chien, *Adv. Mater.* **16**, 61 (2004).
16. During the preparation of this manuscript a patent was published that covers a wide variety of fluoranthenes :D. Florian, R. Reinhold, J. Roesch *PCT Int. Appl.*, 033051 (2005)

Capasso Christy G Civ AFRL/AFOSR

From: Linda Ross [linda@cmliris.harvard.edu]
Sent: Friday, March 24, 2006 3:52 PM
To: AFRL/AFOSR Technical Reports; Gresham Jennifer S Maj AFRL/AFOSR
Subject: Final Technical Report F49620-03-1-0063
Attachments: Lieber_AFOSR_FinalReport_129988.pdf

Maj Jennifer Gresham, PhD
AFOSR Program Manager
Surface & Interfacial Science
875 North Randolph St.
Suite 325, Room 3112
Arlington, VA 22203

Dear Major Jennifer Gresham, PhD,

Re: Award F49620-03-1-0063

Attached please find our Final Report for the AFOSR award entitled "Development and Applications of Nanowire Nanophotonics", for the project period 15 January 2003 through 31 December 2005. I am also sending directly to you by Fedex, 3 hard copies of this report and an electronic copy as .pdf file on CD.

If you would like additional copies, please do not hesitate to ask.

Thank you very much for your time and support of this program.

Best regards,

Charles M. Lieber
Mark Hyman Professor of Chemistry

Linda E. Ross
Laboratory Administrator
Lieber Group, Harvard University
12 Oxford St.
Cambridge, MA 02138
Phone: (617) 384-7701
Fax: (617) 496-5442